

Absolute calibration of the transverse analyzing power in proton-carbon elastic scattering at 50.24 MeV

A. Converse and W. Haeberli

University of Wisconsin, Madison, Wisconsin 53706

W. Hajdas, St. Kistryn,* J. Lang, J. Liechti,† H. Lüscher, R. Müller, J. Smyrski,* and J. Sromicki
Institut für Mittelenergiephysik, Eidgenössische Technische Hochschule, Zürich-Hönggerberg, CH-8093 Zürich, Switzerland

(Received 25 November 1991)

To provide an accurately calibrated polarization analyzer, the analyzing power for elastic scattering of protons from natural carbon at $E_{\text{lab}} = 50.24$ MeV and $\theta_{\text{lab}} = 50.0^\circ$ was measured by scattering protons of very high and precisely known polarization (0.9965 ± 0.0007) from a graphite target. The result of the calibration is $A = 0.9277 \pm 0.0036$, where the error is the quadratic sum of the statistical error ± 0.0033 and systematic uncertainties which total ± 0.0016 .

PACS number(s): 25.40.Cm, 24.70.+s

I. INTRODUCTION

Modern sources of polarized ions provide intensities of a microampere or more. Consequently, knowledge of the beam polarization, rather than statistical uncertainty, often limits the accuracy of studies of spin effects in nuclear scattering. For instance, a recent measurement [1] of the angular distribution of the analyzing power A in 50 MeV proton-proton scattering achieved a statistical precision of $\Delta A / A = 0.005$, but its usefulness in determining p - p phase shifts is lessened by the overall scale uncertainty of 2% stemming from the uncertainty in previously published proton-carbon polarization standards. Here we report a study of the elastic scattering of 50 MeV protons from natural carbon, intended to provide a more accurate calibration. The experiment made use of a novel double scattering technique to achieve an absolute accuracy of better than 0.004.

II. METHOD

The method used in this experiment is described in more detail elsewhere [2], but in this section we sketch the essential points. As shown in Fig. 1, a primary beam of transversely polarized protons is scattered from target T_1 and then from target T_2 whose analyzing power is to be measured. With the appropriate choice for the first target, a secondary beam with high and extremely well-known polarization is obtained. The analyzing power of the second target is then equal to the asymmetry of the protons scattered from that target normalized to the secondary beam polarization.

Given a primary beam of spin- $\frac{1}{2}$ particles with polarization p incident on a spin-0 target with analyzing power A_1 , the polarization p' of the resulting secondary beam is given by [3]

$$p' = \frac{p + A_1}{1 + pA_1}. \quad (1)$$

Then, with only moderately accurate knowledge of the primary beam polarization and first target analyzing power, and provided that they are both large ($\gtrsim 0.9$), we achieve very accurate knowledge of the secondary beam polarization. For example, if $A_1 = 0.900 \pm 0.020$ and $p = 0.900 \pm 0.020$, then $p' = 0.9945 \pm 0.0016$.

In this method, the left-right asymmetry ϵ_2 of protons scattered elastically from the second target is determined:

$$\epsilon_2 \equiv \frac{N_L - N_R}{N_L + N_R}. \quad (2)$$

Here N_L and N_R are the number of protons detected in the left and right detectors with spin-up primary beam. Aside from corrections discussed below, the analyzing power of the second target is then given by

$$A_2 = \epsilon_2 / p'. \quad (3)$$

III. APPARATUS

The cyclotron at the Paul Scherrer Institute provided a beam of protons with mean energy 54.75 ± 0.06 MeV and intensity $1-2 \mu\text{A}$. We continuously monitored the beam polarization with a polarimeter located upstream of the double scattering apparatus. This polarimeter consisted of a $200 \mu\text{g}/\text{cm}^2$ carbon foil (T_0) and NaI detectors with 3 mm diameter collimators positioned 210 mm from the

*Present address: Institute of Physics, Jagellonian University, 30059 Cracow, Poland.

†Present address: Dr. Graf AG, CH-4563 Gerlafingen, Switzerland.

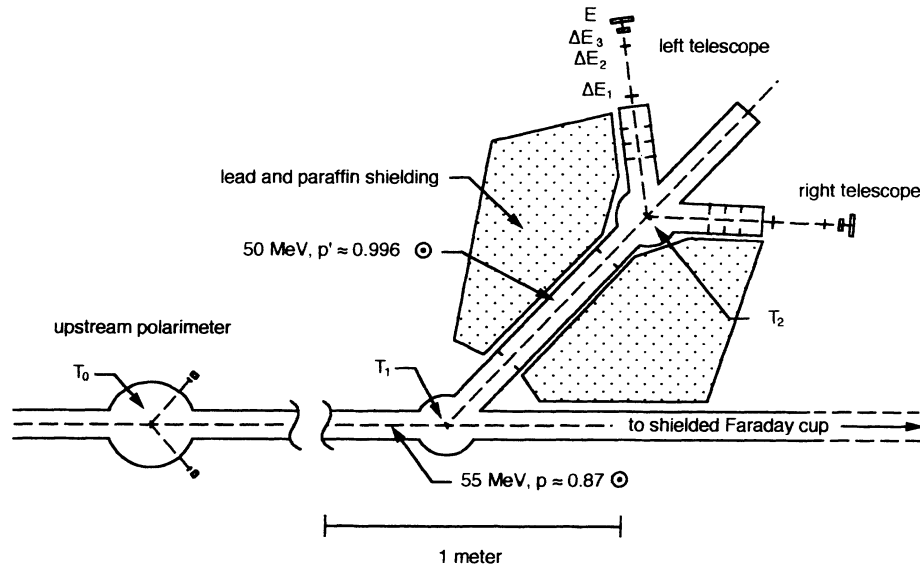


FIG. 1. Scale drawing of the apparatus (top view).

foil and 50° left and right of the beam axis. Only data taken with spin-up beam were used in the analysis of the double scattering experiment. However, the determination of the beam polarization from the upstream polarimeter required two spin states, so we cyclically directed the polarization up for 0.9 s and then down for 0.1 s. The beam diameter was 2 mm at the first graphite target T_1 . Scattered protons continued 100 cm in vacuum to the 50 mm high and 30 mm wide second target T_2 , which was suspended by a 3 mm wide graphite strip. The center of this target was 47.5° to the left of the primary beam axis, at the maximum of the analyzing power at 54 MeV, thus maximizing p' and minimizing its error. Both targets were 90.6 ± 3.0 mg/cm² thick. The normal to the first target formed an angle of 24° with the cyclotron beam axis, minimizing path length differences within the graphite and thus reducing the energy spread of the secondary beam.

Protons that scattered from the second target traveled an additional 40 cm in vacuum and exited through $25 \mu\text{m}$ Mylar windows. Four-element scintillator detector telescopes were located $50.03^\circ \pm 0.10^\circ$ left and right of the axis defined by the two targets. The protons passed through three plastic scintillators with thicknesses 1.0 mm (ΔE_1), 1.0 mm (ΔE_2), and 12.5 mm (ΔE_3); they stopped in 12.5 mm thick NaI scintillators (E). The 28.0 mm diameter ΔE_2 detectors, placed 60 cm from the second target, defined the solid angles of the telescopes. The ΔE_3 and E detectors were large enough to catch all multiply-scattered protons. For each quadruple coincidence, the pulse heights from the ΔE_2 , ΔE_3 , and E detectors and the time of flight between ΔE_2 and ΔE_3 were recorded in event mode. We used ΔE_1 for coincidences only and did not record the pulse height from this detector. We checked periodically that the discriminator triggered by the ΔE_1 detector was set well below the lower edge of the proton peak.

IV. ANALYSIS

A. Raw asymmetry

In 45 hours of data taking, we observed a total of ≈ 17000 events in the two detector telescopes in which protons were scattered elastically while the beam polarization was directed upward. Figure 2 shows samples of the data collected. The time-of-flight (TOF) spectrum is very clean: the intensity of the flat background, used for subtraction of accidental coincidences, is a few parts per 10^3 of that of the main peak. The energy resolution of the angle defining detector ΔE_2 is poor, as expected for such a thin scintillator. The ΔE_3 detector was intentionally made thick to provide rough discrimination between elastic and inelastic events. Due to the energy dependence of the stopping power, higher energy protons produce less light in this detector and therefore the elastic peak appears to the left of the inelastic peak.

The first part of the analysis of the double scattering data consisted of projecting the 4-parameter events onto the pulse-height spectrum of the stopping detector (E). As seen in Fig. 2, wide cuts were used for the TOF and ΔE_2 spectra. For the ΔE_3 detector, conservative limits were used with the upper cut set several half-widths above the centroid of the elastic scattering peak. In this way we assure that no elastic scattering events were lost in the analysis. With the cuts indicated in Fig. 2 we obtained the E spectra shown in Fig. 3. A clean valley separates elastic events from inelastic scattering. To account for a 3% drift in the gain of the photomultipliers over the course of the measurement, the integration limits were fixed with respect to the centroid of the elastic peaks in the E -detector spectra for each 8-hour set of runs. We checked that variations in the cuts did not affect our results. To suppress systematic effects, we interchanged the positions of the two telescopes at regular

intervals. The results from these two configurations were statistically consistent. The left-right asymmetry measured in the elastic peaks in the E spectra was 0.9108 ± 0.0032 .

The determination of A_2 from this measured asymmetry is summarized in Table I and will now be described in detail.

B. Secondary beam polarization

Because a small fraction f of the protons were scattered in the first target by ^{13}C (spin- $\frac{1}{2}$), the secondary

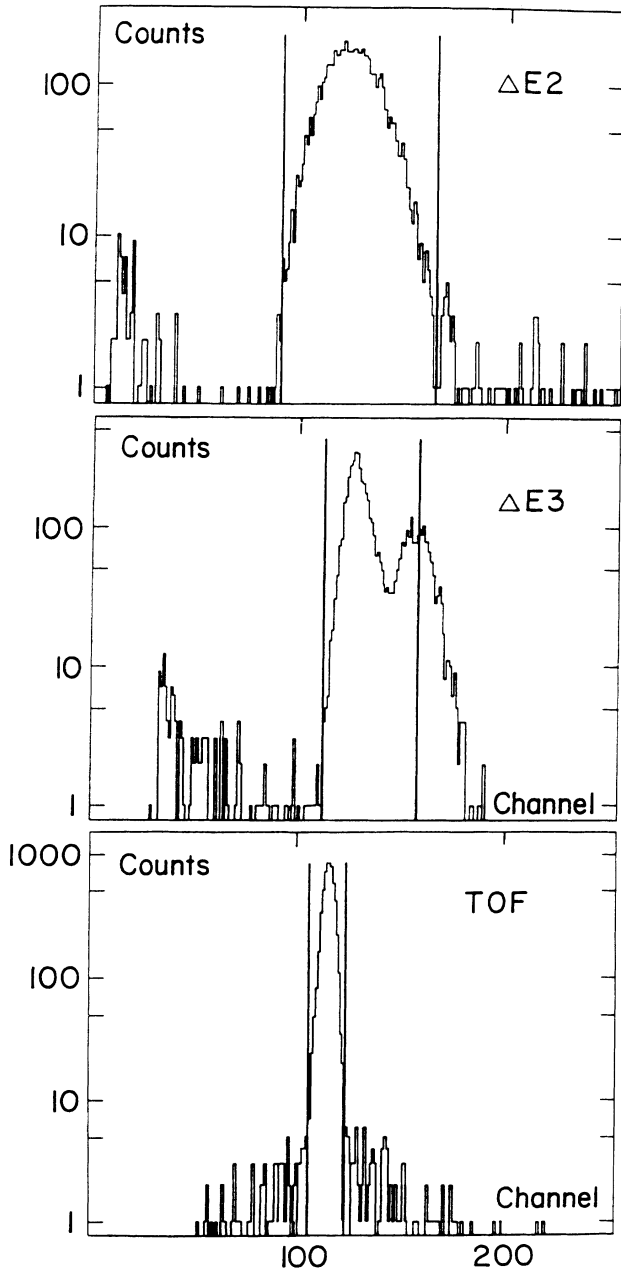


FIG. 2. Spectra from the left telescope showing cuts used in sorting.

beam polarization is not simply given by Eq. (1) which applies to a spin-0 target, but instead by [3]

$$p' = (1-f) \frac{p^+ + A_1^{(12)}}{1 + p^+ A_1^{(12)}} + f \frac{p^+ D + A_1^{(13)}}{1 + p^+ A_1^{(13)}}, \quad (4)$$

where D is the depolarization parameter in p - ^{13}C scattering. Table II summarizes the calculation of p' . In Eq. (4) f is the product of the abundance of ^{13}C in natural carbon [4] (0.0111 ± 0.0005) and the ratio of the p - ^{13}C to p - ^{12}C cross sections at 47.5° . The measured ratio at [5] 33 MeV is 0.936 ± 0.020 and at [6] 72 MeV it is 0.990 ± 0.024 ; consequently, we use $f = 0.0106 \pm 0.0006$. Based on two measurements, $D(65 \text{ MeV}, 45^\circ) = 0.952 \pm 0.023$ [7] and $D(72 \text{ MeV}, 63^\circ) = 0.977 \pm 0.004$ [8], we conservatively assume $D \geq 0.9$. By its definition D is bound from above by one. Therefore, in the calculation of p' we use $D = 0.95 \pm 0.05$. The analyzing power for scattering from ^{13}C in the first target

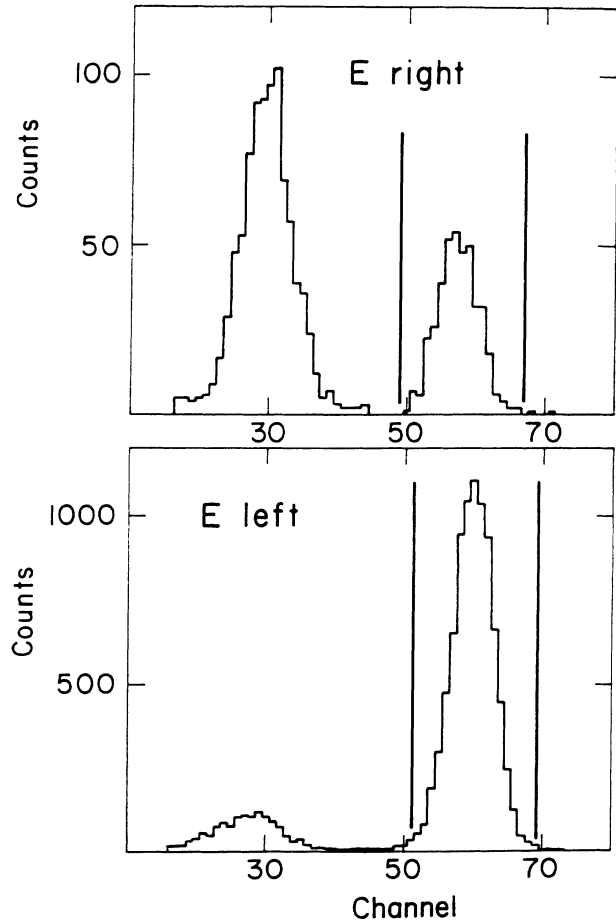


FIG. 3. Total data from the E detectors at the left and the right after sorting with the cuts shown in Fig. 2. The higher energy peaks are from elastic scattering and the lower energy peaks contain protons which scattered inelastically from a carbon nucleus leaving it in the first excited state at 4.44 MeV. Sums within the markers shown were used to calculate the raw asymmetry.

TABLE I. Corrections applied to the measured asymmetry and the resulting value of the transverse analyzing power for elastic scattering of protons from natural carbon. Systematic uncertainties are added in quadrature to the statistical uncertainties.

Measured asymmetry (statistical uncertainty only)		0.9108±0.0032
Secondary beam polarization	+0.0033±0.0007	
Finite solid angle	+0.0087±0.0005	
Double scattering in the second target	+0.0039±0.0006	
Accidental coincidences and room background	+0.0008±0.0008	
Pileup	+0.0000± $\begin{smallmatrix} 0.0002 \\ 0.0000 \end{smallmatrix}$	
Target contaminants	+0.0000± $\begin{smallmatrix} 0.0005 \\ 0.0000 \end{smallmatrix}$	
Difference in detector solid angles	+0.0000±0.0003	
Angle of second scattering	+0.0000±0.0003	
Energy of second scattering	+0.0002±0.0007	
Sum of systematic corrections		+0.0169±0.0016
$A(E_{\text{lab}} = 50.24 \text{ MeV}, \theta_{\text{lab}} = 50.0^\circ) =$		0.9277±0.0036

at 54.2 MeV and 47.5° was determined in a separate measurement. A 150±50 mg/cm² and 89±2% isotopically enriched ¹³C target was used in place of the polarimeter target (T_0). The result was $A_1^{(13)} = 0.933 \pm 0.015$.

We determine the analyzing power for scattering from ¹²C in the first target using the following procedure: As a first approximation we insert into Eq. (4) the previously published value [9] $A(54.4 \text{ MeV}, 47.5^\circ) = 0.956 \pm 0.016$ whose error is dominated by an overall scale uncertainty. This rough value for $A_1^{(12)}$ yields a preliminary value for the secondary beam polarization p' with an uncertainty ±0.0011. To further reduce the error in $A_1^{(12)}$ we calculate a preliminary value for A_2 , which we use to reduce the normalization error of the data from Ref. [9]. This rescaling procedure together with small corrections for ¹³C and the beam energy yields the value $A_1^{(12)} = 0.957 \pm 0.008$.

The cyclotron beam polarization in the spin-up state, p^+ in Eq. (4), is calculated from the upstream polarimeter data. We obtain four count rates from the upstream polarimeter detectors:

$$N_L^+ \propto (1 + p^+ A_0) \Omega_L, \quad (5)$$

$$N_L^- \propto (1 - p^- A_0) \Omega_L, \quad (6)$$

$$N_R^+ \propto (1 - p^+ A_0) \Omega_R, \quad (7)$$

$$N_R^- \propto (1 + p^- A_0) \Omega_R, \quad (8)$$

where p^+ and p^- are the magnitudes of the cyclotron beam polarization in the + and - states, Ω_L and Ω_R are the left and right polarimeter detector solid angles, and

A_0 is the natural carbon analyzing power for elastic scattering from the polarimeter target at 50° and 54.8 MeV. In the formulas above all common factors have been omitted. The ratio of beam currents for the two spin states is known [1] to differ from one by less than 0.002, which corresponds to a negligible uncertainty in the analysis of the beam polarization. Though it is not the peak in the angular distribution at 54.8 MeV, we set the polarimeter detectors to the same angle as the double scattering calibration. This allowed us to use the preliminary value of A_2 mentioned above to normalize the energy dependence taken from Ref. [9] without an additional adjustment for the angular dependence. We obtain $A_0 = 0.953 \pm 0.010$. The asymmetries measured in the polarimeter were

$$\epsilon_L \equiv \frac{N_L^+ - N_L^-}{N_L^+ + N_L^-} = 0.8316 \pm 0.0005 \quad (9)$$

and

$$\epsilon_R \equiv \frac{N_R^+ - N_R^-}{N_R^+ + N_R^-} = -0.8303 \pm 0.0005. \quad (10)$$

The beam polarization p^+ can be expressed in terms of these quantities as

$$p^+ = \frac{\epsilon_L + \epsilon_R + 2\epsilon_L\epsilon_R}{A_0(\epsilon_R - \epsilon_L)} = 0.871 \pm 0.009. \quad (11)$$

Systematic uncertainties in the evaluation of p^+ arise from corrections for angle and energy averaging and cali-

TABLE II. Calculation of the secondary beam polarization p' .

Parameter	Value	Corresponding uncertainty in p'
Cyclotron beam polarization	$p^+ = 0.8709 \pm 0.0092$	±0.00023
$p^{12}\text{C}$ analyzing power	$A_1^{(12)} = 0.9573 \pm 0.0077$	±0.00055
Fraction scattered from ¹³ C	$f = 0.0106 \pm 0.0006$	±0.00002
$p^{13}\text{C}$ analyzing power	$A_1^{(13)} = 0.933 \pm 0.015$	±0.00001
$p^{13}\text{C}$ depolarization parameter	$D = 0.95 \pm 0.05$	±0.00027
Double scattering correction	-0.00025 ± 0.00010	±0.00010
Secondary beam polarization		$p' = 0.99646 \pm 0.00066$

brations, spin-correlated gain shifts in the polarimeter detectors, and background. These sources taken together contribute <0.0001 to the uncertainty in the secondary beam polarization.

A calculation based on the angular distribution of A_0 and σ of Ref. [9] shows that large-angle double scattering within the first target, similar to that within the second target discussed in the following section, reduced p' by 0.0002 ± 0.0001 .

We conclude that the mean secondary beam polarization in this experiment was $p' = 0.9965 \pm 0.0007$.

C. Large corrections ($> 1\sigma$)

Two geometrical corrections applied to the measured asymmetry are relatively large. However, the uncertainties associated with these corrections are well below the final error of this calibration.

1. Angle averaging

We measured the analyzing power near the peak in its angular distribution, but, because of the finite extent of the second target and the defining detectors, we collected protons which scattered through a range of angles around 50° . The acceptance function of the system, with FWHM of 3° , is shown in Fig. 4. We calculate the difference between the asymmetry resulting from this

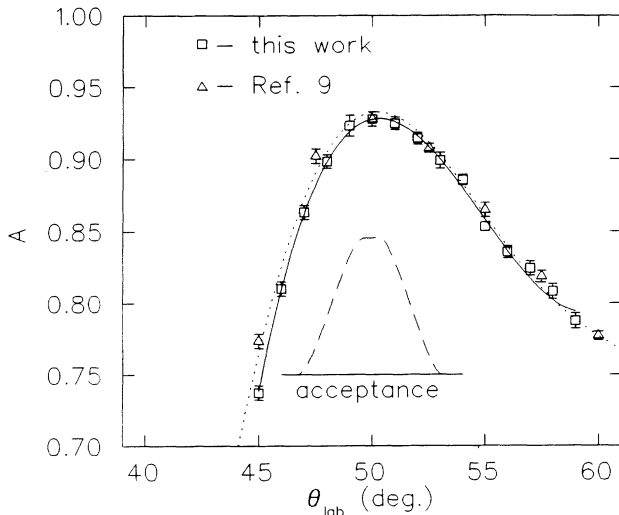


FIG. 4. The angular distribution of A . The dashed curve represents the geometrical acceptance of the double scattering apparatus. \square , our measurement of A at 50.39 MeV (see Table III). \triangle , the measurement of A at 49.6 MeV and has been scaled to 50.4 MeV using a cubic fit to the energy dependence also found in Ref. [9]. Both sets of data have been normalized using the result of the present absolute calibration to 0.9292 at 50° . There is an overall scale uncertainty of 0.39%. The dotted curve is a quintic fit to the data of Ref. [9] over the range $37.5^\circ \leq \theta_{\text{lab}} \leq 65.0^\circ$. The solid curve is a cubic fit to our data which we used for the solid angle correction described in the text. The value of $A(50.24 \text{ MeV}, 50.0^\circ)$ obtained with the correction using the data of Ref. [9] differs from our reported value by 0.00025, or 0.07σ .

finite geometry and the asymmetry expected with point targets and detectors. We account for the vertical and horizontal dimensions of the second target and the detectors and the reduced effective polarization of protons which scattered out of the horizontal plane.

The calculation involves numerical integration of the products of relative angular distributions of p - C cross sections and analyzing powers both for scattering from the first target ($E = 54 \text{ MeV}$) and from the second target ($E = 50 \text{ MeV}$). We use the measurements of Ref. [9] for $A(54 \text{ MeV}, \theta)$, $\sigma(54 \text{ MeV}, \theta)$, and $\sigma(50 \text{ MeV}, \theta)$. The calculation is most sensitive to $A(50 \text{ MeV}, \theta)$, so to obtain sufficient accuracy we measured this distribution by degrading the 55 MeV cyclotron beam to 50 MeV. The results of this measurement, corrected for angular resolution and background, are shown in Table III and Fig. 4. Finite geometry reduced the measured asymmetry by 0.0087 ± 0.0005 compared to the expected asymmetry for the central path.

2. Large-angle double scattering within the second target

While we used a relatively thick second target, we wish to deduce the analyzing power expected from a thin target in which large-angle double scattering is negligible. Calculations of this effect with numerical integration over the distributions $A(\theta)$ and $\sigma(\theta)$ of Ref. [9] show that events in which a proton scattered from two nuclei in target T_2 reduced the measured asymmetry by 0.0039 ± 0.0006 .

D. Small corrections and uncertainties ($< \frac{1}{4}\sigma$)

Because of the high asymmetry (≈ 0.91) in scattering from the analyzing target T_2 , we were particularly sensitive to background in the right-hand detector telescope where a total of 756 elastically scattered protons were ob-

TABLE III. Relative angular distribution of the transverse analyzing power in elastic scattering of protons from natural carbon at $E_{\text{lab}} = 50.39 \text{ MeV}$. The data are normalized to 0.9292 at 50° using the result of the present absolute calibration. There is an additional scale uncertainty of 0.39%.

θ_{lab} (deg)	A	ΔA
45.0	0.7383	0.0050
46.0	0.8111	0.0050
47.0	0.8643	0.0048
48.0	0.8998	0.0047
49.0	0.9246	0.0072
50.0	0.9292	0.0051
51.0	0.9261	0.0044
52.0	0.9157	0.0040
53.0	0.9004	0.0056
54.0	0.8868	0.0037
55.0	0.8544	0.0029
56.0	0.8369	0.0042
57.0	0.8256	0.0049
58.0	0.8093	0.0053
59.0	0.7887	0.0054

served. Thus, for instance, an uncertainty of eight counts out of these 756 contributes 0.001 to ΔA_2 .

1. Accidental coincidences and room background

To check for accidental background, broad cuts were set in the flat portion of the TOF spectrum to the left and right of the peak, leaving all other cuts as in the main analysis (see Fig. 2). The events projected onto the pulse-height spectra of the E detectors were then normalized by the ratio of the widths of the time-to-amplitude converter windows used in these two procedures. Accidental background was found to be negligible with an uncertainty in A_2 of ± 0.0002 .

To determine background from such mechanisms as neutrons produced in the first target or the beam dump, which travel directly to the scintillators and knock-out high energy protons, we devoted one-fifth of the running time to a measurement with the second target removed. We found one count on the low counting-rate side (see Fig. 3) compatible with such a mechanism. This corresponds to a 0.0008 ± 0.0008 correction to the measured analyzing power.

2. Pileup

To ensure that we did not count inelastically scattered protons that pileup had pushed into the elastic peak, we needed a wide gap in the pulse-height spectrum of the E detector between the ground state and first excited state peaks. We observed no counts in the gap between the elastic and inelastic scattering peaks in the E spectrum of the right-hand telescope (Fig. 3). Conservatively assuming the pileup energy distribution to be flat, we expect that less than three counts due to pileup lie beneath the elastic peak. This corresponds to an uncertainty of < 0.0002 in A_2 due to pileup.

3. Chemical contaminants in the second target

Based on atomic absorption spectroscopy, ash tests, and x-ray fluorescence measurements, the manufacturer stated that the natural carbon targets [10] were pure to 5 ppm with the main contaminant usually being silicon. Though we baked the targets for 11 hours at 150°C we feared contamination from oxygen in absorbed water. As an additional check we obtained upper limits on possible chemical contaminants by scattering 72 MeV protons to 90° . To obtain adequate energy resolution we used 0.1 mm graphite targets instead of the 0.5 mm plates of the same material used in the analyzing power measurement.

In this auxiliary measurement we observed $\approx 35\,000$ counts in the elastic carbon peak compared to eight counts compatible with scattering from ^{16}O , four counts compatible with scattering from heavier nuclei, and six counts (calculated to be consistent with pileup) above the beam energy of 72 MeV. We analyze this measurement assuming the ‘‘contaminant’’ counts came from ^{16}O and any combination of ^{24}Mg , ^{28}Si , or ^{40}Ca . Using measurements [7,11–14] and optical model predictions [15] of cross sections, we scale the measured counts by the ratio $\sigma(50\text{ MeV}, 50^\circ)/\sigma(72\text{ MeV}, 90^\circ)$ and adjust for the mea-

sured analyzing powers [7,16–18] of the contaminants. We conclude that the resulting correction to A_2 is less than 0.0005. Because the counts identified as contaminants could also have been pileup, this is a conservative upper limit.

4. Detector solid angles and positions

A difference in the solid angles subtended by the defining detectors (ΔE_2) of the two telescopes produces a false asymmetry. We measured the solid angles of the defining detectors as viewed from the second target and found $|\Omega_1/\Omega_2 - 1| < 0.006$. The effect was partially reduced by physically interchanging the two telescopes at regular intervals. This limits the uncertainty in A_2 due to solid angle differences to < 0.0003 . The defining detectors were positioned with 0.1° accuracy which corresponds to an uncertainty in A_2 of 0.0003.

5. Energy at second scattering

Using a recent calibration of the cyclotron’s analyzing magnet [19] we determined the mean beam energy to one part per 10^3 . We checked predictions [20] of energy loss in the targets by placing a detector in the secondary beam and observing the shift of the elastic scattering peak as we inserted different thicknesses of target material in front of the detector. Energy losses in the range 0.5–5.0 MeV were measured, and the 4.44 MeV separation between the ground state and first excited state peaks served as a calibration. The predictions and measurements agreed to 2% which we take as the uncertainty in the energy loss: 1.563 ± 0.031 MeV. We conclude that the mean energy of the protons as they scattered in the second target was 50.24 ± 0.08 MeV. Given the energy dependence described in Table IV, this corresponds to an uncertainty in A_2 of 0.0007. Averaging over the energy spread in the targets due to straggling and different path lengths and over the spread in the cyclotron beam energy introduces a correction of 0.0002 to A_2 with an uncertainty < 0.0001 .

V. CONCLUSION

We have applied a new method to measure the transverse analyzing power in elastic scattering of protons from natural carbon at 50.24 MeV and 50.0° . The analysis of our data, summarized in Table I, yields $A = 0.9277 \pm 0.0036$, where the error is the quadratic sum of the statistical error of ± 0.0033 and the systematic errors which total ± 0.0016 . This value, corrected for the energy dependence around 50 MeV, agrees well with the previously published absolute calibration $A(49.7\text{ MeV}, 50.0^\circ) = 0.919 \pm 0.018$ [21]. The new result is five times more precise.

In our analysis we considered a number of systematic effects, which might be important at this level of accuracy. The largest corrections are due to the finite solid angles of the detectors and multiple scattering in the thick second target. Such corrections cannot be avoided in any double scattering experiment with high statistical preci-

TABLE IV. Fits to the energy and angle dependence of the p -carbon elastic scattering analyzing power: $A(\bar{E}, 50.0^\circ) = \sum_{i=0, \dots, 2} a_i \bar{E}^i$, $\bar{E} = (E - 50.24 \text{ MeV}) / (5.0 \text{ MeV})$, and $A(50.39 \text{ MeV}, \bar{\theta}) = \sum_{i=0, \dots, 3} b_i \bar{\theta}^i$, $\bar{\theta} = (\theta - 50.0^\circ) / 5.0^\circ$, where E is the laboratory energy of the incident proton measured in MeV, and θ is the laboratory angle of the scattered proton measured in degrees. The data of Ref. [9] have been used for the energy dependence, and the data in Table III have been used for the angular dependence. Using the present absolute calibration, the energy distribution has been normalized to 0.9277 at 50.24 MeV, and the angular distribution to 0.9292 at 50.0° . The uncertainties in the quadratic coefficients provide good approximations to the errors in the fits calculated exactly with the full covariance matrices scaled by $\chi^2/\text{D.F.}$

	Energy	Angle
Range of data used in fit	$39.6 \text{ MeV} \leq E \leq 59.5 \text{ MeV}$	$45.0^\circ \leq \theta \leq 59.0^\circ$
Degrees of freedom of fit	2	11
$\chi^2/\text{D.F.}$ of fit	5.8	0.98
Best-fit parameters	$a_0 = 0.9277 \pm 0.0036$ $a_1 = 0.0493$ $a_2 = -0.0224 \pm 0.0029$	$b_0 = 0.9292 \pm 0.0036$ $b_1 = 0.0156$ $b_2 = -0.0130 \pm 0.0034$ $b_3 = 0.0443$
Estimate of uncertainty		
Valid in the range	$45 \text{ MeV} \leq E \leq 55 \text{ MeV}$	$45^\circ \leq \theta \leq 55^\circ$

cision. For other effects we provided upper limits on the level of a few times 10^{-4} .

Table IV presents the results of a cubic fit to our measurement of the angular distribution $A(50.39 \text{ MeV}, \theta)$ and a quadratic fit to the energy distribution $A(E, 50.0^\circ)$ taken from Ref. [9]. For example, we estimate $A(50.06 \text{ MeV}, 50.3^\circ) = 0.9264 \pm 0.0036$. As a consequence of this the high precision pp analyzing power data of Ref. [1] should all be renormalized by the factor 1.0069 ± 0.0039 .

The discussed procedure for measuring absolute analyzing powers is based on the idea of producing a secondary beam of very accurately determined polarization and measuring the left-right asymmetry in the scattering of this beam. This simple method can provide very high precision polarization standards. This is possible due to suppression of statistical as well as some systematic effects in the regime where analyzing powers are large [2]. Recently, the absolute analyzing power for elastic scattering of protons has also been measured at two other energies [22,23]. The three apparently different methods rely on very similar physical principles and, as a consequence, all of them work particularly well for high

analyzing powers. (The error scales approximately with $[2] 1 - A^2$.)

In this measurement the statistical accuracy could have been improved by using a magnetic focusing device between the first and second targets. However, the method used here has the advantage that in the calculation of the geometrical corrections the trajectories of the particles can be represented by straight lines. While the method presented is insensitive to uncertainties in the polarization of the primary beam and in the analyzing power of the first target, care must be taken to eliminate background radiation on the low counting-rate side of the double scattering apparatus.

ACKNOWLEDGMENTS

We are grateful to Dr. R. Henneck for the ^{13}C target, to Dr. M. Simonius for useful discussions, and to the PSI cyclotron staff for a high quality beam. This work was supported by the Swiss National Foundation and the United States National Science Foundation.

- [1] J. Smyrski, St. Kistryn, J. Lang, J. Liehti, H. Lüscher, Th. Maier, R. Müller, M. Simonius, J. Sromicki, F. Foroughi, and W. Haerberli, Nucl. Phys. **A501**, 319 (1989).
- [2] J. Sromicki, A. Converse, J. Lang, and R. Müller, Phys. Rev. C **40**, R1111 (1989).
- [3] L. Wolfenstein, Phys. Rev. **96**, 1654 (1954); for modern notation see G. G. Ohlsen, Rep. Prog. Phys. **35**, 717 (1972).
- [4] *Table of Isotopes*, 7th ed., edited by C. Michael Lederer and Virginia S. Shirley (Wiley, New York, 1978), p. 13.
- [5] E. E. Gross, J. J. Malanify, A. van der Woude, and A. Zucker, Phys. Rev. Lett. **21**, 1476 (1968).
- [6] B. von Przewoski, P. D. Eversheim, F. Hinterberger, L. Doberitz, J. Campbell, M. Hammans, R. Henneck, W. Lornzon, M. A. Pickar, and I. Sick, Nucl. Phys. **A496**, 15 (1989).
- [7] Masanobu Nakamura, Harutaka Sakaguchi, Hiroshi Sakamoto, Hidemi Ogawa, Osamu Cynshi, Shinsaku Kobayashi, Syohei Kato, Nobuyuki Matsuoka, Kichiji Hatanaka, and Tetsuo Noro, Nucl. Instrum. Methods **212**, 173 (1983).
- [8] B. v. Przewoski, P. D. Eversheim, F. Hinterberger, U. Lahr, J. Campbell, J. Götz, M. Hammans, R. Henneck, G. Masson, I. Sick, and W. Bauhoff, Phys. Rev. Lett. **64**, 368 (1990).
- [9] M. Ieiri, H. Sakaguchi, M. Nakamura, H. Sakamoto, H. Ogawa, M. Yosoi, T. Ichihara, N. Isshiki, Y. Takeuchi, H. Togawa, T. Tsutsumi, S. Hirata, T. Nakano, S. Kobayashi, T. Noro, and H. Ikegami, Nucl. Instrum. Methods **A257**,

- 253 (1987).
- [10] Type AXF5Q1, POCO graphite, Decatur, Texas 76234.
- [11] J. A. Fannon, E. J. Burge, D. A. Smith, and N. K. Ganguly, *Nucl. Phys.* **A97**, 263 (1967).
- [12] A. A. Rush, E. J. Burge, V. E. Lewis, D. A. Smith, and N. K. Ganguly, *Nucl. Phys.* **A104**, 340 (1967).
- [13] K. Yagi, H. Ejiri, M. Furukawa, Y. Ishizaki, M. Koike, K. Matsuda, Y. Nakajima, I. Nonaka, Y. Saji, E. Tanaka, and G. R. Satchler, *Phys. Lett.* **10**, 186 (1964).
- [14] L. N. Blumberg, E. E. Gross, A. van der Woude, A. Zucker, and R. H. Bassel, *Phys. Rev.* **147**, 812 (1966).
- [15] R. Henneck (private communication).
- [16] N. M. Clarke, E. J. Burge, D. A. Smith, and J. C. Dore, *Nucl. Phys.* **A157**, 145 (1970).
- [17] H. Sakaguchi, M. Nakamura, K. Hatanaka, A. Goto, T. Noro, F. Ohtani, H. Sakamoto, and S. Kobayashi, *Phys. Lett.* **89B**, 40 (1979).
- [18] R. M. Craig, J. C. Dore, J. Lowe, and D. L. Watson, *Nucl. Phys.* **86**, 113 (1966).
- [19] J. Smyrski, Dissertation, Jagellonian University 1988.
- [20] S. Mellema, computer code ELOSS, University of Wisconsin; J. B. Marion and F. C. Young, *Nuclear Reaction Analysis* (North-Holland, Amsterdam, 1968), p. 15.
- [21] Syohei Kato, Kenju Okada, Michiya Kondo, Akira Shimizu, Kazuhiko Hosono, Takane Saito, Nobuyuki Matsuo, Shinji Nagamachi, Keigo Nisimura, Norio Tamura, Kenichi Imai, Kazumi Egawa, Masanobu Nakamura, Tet-suo Noro, Hajime Shimizu, Kouya Ogino, and Yusaku Kadota, *Nucl. Instrum. Methods* **169**, 589 (1980).
- [22] P. D. Eversheim, F. Hinterberger, U. Lahr, B. Von Przewoski, J. Campbell, J. Götz, M. Hammans, R. Henneck, G. Masson, and I. Sick, *Phys. Lett. B* **234**, 253 (1990).
- [23] M. Clajus, P. Egun, W. Gruebler, P. Hautle, A. Weber, P. A. Schmelzbach, W. Kretschmer, M. Haller, C. J. Prenzel, A. Rauscher, W. Schuster, and R. Weidmann, *Nucl. Instrum. Methods* **A281**, 17 (1989).